

Cite this: *Chem. Commun.*, 2011, **47**, 3604–3606

www.rsc.org/chemcomm

Controllable synthesis of Cu-based nanocrystals in ODA solvent†

Dingsheng Wang and Yadong Li*

Received 11th November 2010, Accepted 20th January 2011

DOI: 10.1039/c0cc04902f

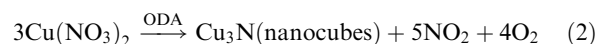
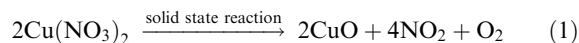
We exploited a solution-based route for preparation of Cu, Cu₂O, Cu₃N, and Cu₂S nanocrystals, that is, direct thermal decomposition of copper salts (Cu(NO₃)₂, CuSO₄) in octa-decylamine (ODA) solvent, which is a novel and ingenious chemical process.

At the nanoscale, materials exhibit interesting size- and shape-dependent properties that differ drastically from those of the bulky materials.¹ Therefore, synthesis of nanomaterials has been among the key research topics in the field of nanoscience and nanotechnology over the past decades.² Cu-based nanomaterials are attracting intense interest from scientists worldwide due to their excellent properties and potential applications.³ For example, Cu nanoparticles show excellent catalytic performance in the methanol reforming process for effective hydrogen production;⁴ comb-like Cu₂O nanorod-based structures were demonstrated to have great application potentials as ethanol sensors;⁵ the utilization of Cu₂S nanocrystals through direct binding with the conductive multiwalled carbon nanotubes could lead to excellent performance of solar cells and the amperometric glucose sensors.⁶

In particular, Cu₃N, as an insulating material with a low reflectivity and high electrical resistivity,^{7–10} holds promise in major applications including high density optical data storage and high-speed integrated circuits.^{11,12} However, in recent years, synthesis of Cu₃N was mainly focused on thin films.^{13,14} There has been a major difficulty in preparing high quality Cu₃N nanocrystals for nano-electronics and optics applications due to the poor thermal stability of Cu₃N and the lack of viable and controllable chemical reactions to produce Cu₃N.¹⁵ So it is necessary to exploit other strategies to synthesize Cu₃N nanocrystals with uniform morphology and size.

As we know, Cu(NO₃)₂ can decompose to CuO *via* a solid state reaction (eqn (1)). However, the decomposition of Cu(NO₃)₂ in ODA solvent is absolutely different from eqn (1). We found that, under proper conditions, Cu₃N could be directly obtained *via* decomposition of Cu(NO₃)₂ (eqn (2)). This chemical reaction is very difficult to be achieved through

solid state processes or other solution routes. Here, the ODA solvent plays a key role in the reduction of Cu₃N products.



In a typical synthesis of Cu₃N, 0.3 g of Cu(NO₃)₂·6H₂O was added into 10 ml of ODA at 240 °C. The reaction finished within 10 min. A powder X-ray diffraction (XRD) experiment was carried out to determine the structure and composition of as-prepared products. As shown in Fig. S1, ESI†, the series of Bragg reflections in the pattern correspond to cubic phase Cu₃N (JCPDS 47-1088), indicating the successful synthesis of Cu₃N *via* the above novel procedure. Fig. 1 shows transmission electron microscope (TEM) and high-resolution TEM (HRTEM) images of as-obtained products. It can be seen that Cu₃N nanocubes are abundantly produced with an average diameter of 15 nm. The selected area electron diffraction (SAED) studies confirm that the nanocubes are single-crystalline and adopt a Cu₃N cubic structure with lattice parameter $a = 0.38$ nm (Fig. 1d). Fig. 1c reveals clear lattice fringes with an interplanar distance of about 0.38 nm which is a characteristic of the cubic Cu₃N crystal phase in the (100)

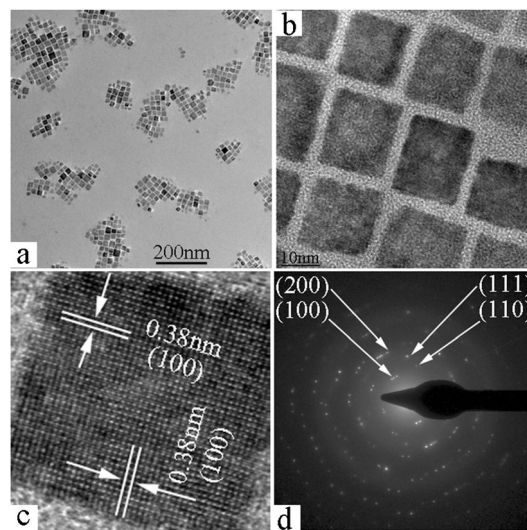


Fig. 1 (a) TEM and (b) HRTEM images of Cu₃N nanocubes. (c) Crystal-lattice image of an individual Cu₃N nanocube. (d) SAED pattern of Cu₃N nanocubes.

Department of Chemistry, Tsinghua University, Beijing, 100084, China. E-mail: ydli@tsinghua.edu.cn; Fax: +86 10-62788765

† Electronic supplementary information (ESI) available: The synthesis details, EDS, XPS, and more XRD patterns and TEM images. See DOI: 10.1039/c0cc04902f

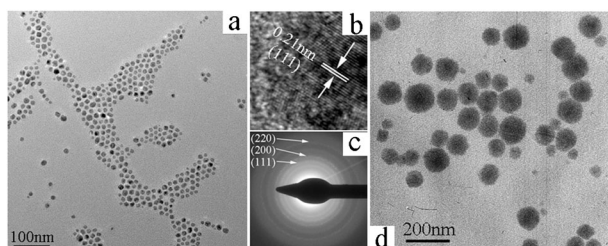


Fig. 2 (a) TEM image of Cu nanocrystals. (b) Crystal-lattice image of an individual Cu nanoparticle. (c) SAED pattern of Cu nanocrystals. (d) TEM image of Cu₂O nanocrystals.

plane. The chemical composition of the nanocubes was further checked by energy dispersive spectroscopy (EDS) and confirmed to be pure Cu₃N (Fig. S1, ESI†). X-Ray photoelectron spectroscopy (XPS) was used to analyze the inorganic component and chemical bonding at the surface (Fig. S2, ESI†). The XPS survey spectrum only shows the peaks of Cu, N, O, and C, illustrating the high purity of the sample. The binding energies of N 1s and Cu 2p₃ are 397.4 and 932.7 eV, respectively, which are undoubtedly in accordance with the standard data of Cu₃N.

We can not only synthesize Cu₃N nanocubes by direct thermal decomposition of Cu(NO₃)₂ in ODA solvent, but also achieve size and shape control of Cu₃N nanocrystals *via* adjusting the reaction parameters including reaction temperature and time. Fig. S4 (ESI†) shows TEM images of Cu₃N nanocrystals with different sizes and morphologies obtained under controlled conditions. When 0.3 g of Cu(NO₃)₂·3H₂O was added into 10 ml of ODA at 280 °C, Cu₃N nanoparticles were obtained after 5 min. Fig. S4a (ESI†) displays that their average size is 10 nm. Higher decomposition temperature and shorter reaction time could accelerate the nucleation process and limit the growth process of nanocrystals, leading to the formation of Cu₃N nanoparticles with smaller size. When 0.3 g of Cu(NO₃)₂·3H₂O was reacted first at 260 °C for 5 min and then at 240 °C for another 5 min, Cu₃N nanopolyhedrons with an average size of 15 nm were obtained (Fig. S4b, ESI†). We can see that they are likely to evolve into cubes (some rectangles can be detected). Fig. S4c (ESI†) shows a TEM image of Cu₃N nanoparticles with an average size of 15 nm obtained when 0.3 g of Cu(NO₃)₂·3H₂O was reacted first at 220 °C for 5 min and then at 240 °C for another 5 min. When the reaction was performed at a lower temperature (220 °C) and for a longer time (20 min), a slow nucleation process and a continuous growth process of nanocrystals led to the formation of Cu₃N nanospheres with a larger size of about 50 nm (Fig. S4d, ESI†). Fig. S5 (ESI†) shows the XRD patterns of the series of samples, which confirm that all of the synthesized products are cubic phase Cu₃N. However, there is a small difference in the intensity of diffraction peaks among them. For Cu₃N nanopolyhedrons, the intensity of the (100) peak is little stronger than that of the (111) peak. While for Cu₃N nanoparticles and nanospheres, the intensities of these two peaks are nearly the same. Comparatively, it is obvious that the intensity of the (100) peak of Cu₃N nanocubes (Fig. S1, ESI†) is much stronger than that of the (111) peak. This result demonstrates that the as-obtained

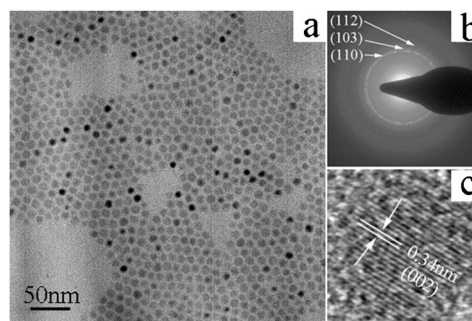
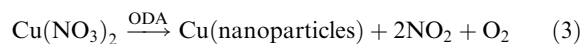


Fig. 3 (a) TEM image of Cu₂S nanocrystals. (b) SAED pattern of Cu₂S nanocrystals. (c) Crystal-lattice image of an individual Cu₂S nanoparticle.

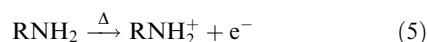
Cu₃N nanocubes expose the (100) crystal plane, which is consistent with the cube-morphology and the above analytic result of HRTEM.

On the other hand, the mole ratio of Cu(NO₃)₂/ODA determines the decomposed products of Cu(NO₃)₂ in the ODA system, and Cu₃N can be obtained only when the ratio is 3 : 80. When the ratio is 1 : 80, Cu nanoparticles are synthesized instead (eqn (3)). Fig. S1 (ESI†) shows the XRD pattern of the products. The peaks at 43.3°, 50.4°, and 74.1° 2θ correspond to the (111), (200), and (220) reflections of face-centered cubic (fcc) structured Cu, respectively (JCPDS 04-0836). The typical TEM image depicted in Fig. 2a displays the nearly monodisperse particle size distribution, and the average diameter of as-prepared Cu particles is 10 nm (Fig. 2b and c). When the ratio is 1 : 8, Cu₂O nanocrystals are the decomposed products of Cu(NO₃)₂ (eqn (4)). The XRD pattern (Fig. S1, ESI†) confirms the formation of Cu₂O in our synthesis. All characteristic peaks match exactly with the standard JCPDS card 65-3288 of cubic Cu₂O. The TEM image (Fig. 2d) shows that the as-obtained Cu₂O nanocrystals exhibit spherical morphology and their diameters range from 50 to 100 nm. If the Cu(NO₃)₂/ODA ratio is between 1 : 80 and 3 : 80, we can't obtain pure products. For example, when the ratio is 2 : 80, a mixture of Cu and Cu₃N was produced (Fig. S6, ESI†). Similarly, when the ratio is 3 : 40, a mixture of Cu₃N and Cu₂O was produced (Fig. S6, ESI†). Therefore, Cu, Cu₃N and Cu₂O nanocrystals can be easily synthesized *via* direct thermal decomposition of Cu(NO₃)₂·3H₂O in ODA solvent under controlled conditions. These obtained nanocrystals can be dispersed in nonpolar solvents (such as cyclohexane or chloroform) to form homogenous colloidal solutions, which are usually stable for months. Fig. S7 (ESI†) shows the visible absorption spectra of as-obtained samples dispersed in cyclohexane. From the visual images of these transparent solutions (Fig. S7, insets, ESI†), we can observe very pure and brilliant colors (especially for Cu₃N).



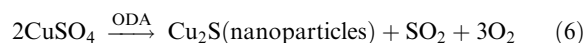
Why is the decomposing reaction of Cu(NO₃)₂ in ODA solvent (eqn (2–4)) abnormal compared to that in solid state

(eqn (1))? In ODA solvent, as shown in eqn (5),¹⁶ ODA can offer electrons which can change the decomposing routes of $\text{Cu}(\text{NO}_3)_2$. In the ingenious process of Cu_3N formation, ODA plays the role of transferring electrons from O^{2-} to Cu^{2+} and N^{5+} as described in Fig. S8†. Cu^{2+} and N^{5+} can't obtain electrons directly from O^{2-} due to a potential barrier. However, they can obtain electrons from ODA. Once ODA loses electrons, ODA^+ is immediately neutralized by electrons offered by O^{2-} . The continuous supply of electrons from ODA to Cu^{2+} and N^{5+} makes the shift of electrons from O^{2-} to ODA to occur continuously, until Cu_3N forms. Three parameters determine whether N^{5+} can be reduced to N^{3-} : ODA, Cu^{2+} , and the $\text{Cu}^{2+}/\text{ODA}$ ratio. Firstly, ODA solvent is indispensable to synthesize Cu_3N from decomposition of $\text{Cu}(\text{NO}_3)_2$. Secondly, among all metal nitrates, only $\text{Cu}(\text{NO}_3)_2$ can decompose to Cu_3N . For AgNO_3 and $\text{Ni}(\text{NO}_3)_2$, Ag^+ can attract electrons from ODA and is reduced to Ag ,¹⁷ while Ni^{2+} can't attract electrons from ODA and thus NiO is the product.¹⁸ The ability of a Cu atom to attract electrons to itself is just between that of Ni and Ag atoms.¹⁹ Therefore, Cu^{2+} can be reduced to Cu^+ and meanwhile induce the reduction of N^{5+} to N^{3-} . Thirdly, the mole ratio of $\text{Cu}^{2+}/\text{ODA}$ is another crucial parameter. We consider that the $\text{Cu}^{2+}/\text{ODA}$ ratio is related to the potential barrier of the $\text{Cu}(\text{NO}_3)_2$ decomposition reaction. Cu^{2+} and N^{5+} can be co-reduced only when the $\text{Cu}^{2+}/\text{ODA}$ ratio is appropriate to just overcome the potential barrier of reaction (2). When the $\text{Cu}^{2+}/\text{ODA}$ ratio decreases, Cu^{2+} can attract enough electrons to be reduced to Cu. When the $\text{Cu}^{2+}/\text{ODA}$ ratio increases, Cu^{2+} can only attract electrons to be reduced to Cu^+ and can't induce the reduction of N^{5+} to N^{3-} .



In the reduction process of $\text{Cu}(\text{NO}_3)_2$ in ODA solvent, although ODA offers electrons, it doesn't participate in the reaction. Taking formation of Cu_3N as an example, ODA offers electrons to Cu^{2+} and N^{5+} , and meanwhile is compensated by electrons from O^{2-} . Actually, ODA is an intermedium that transfers electrons from O^{2-} to Cu^{2+} and N^{5+} , and plays a role similar to that of a "catalyst". Therefore, the N element in Cu_3N doesn't come from ODA. In order to confirm this viewpoint, we changed the reaction precursor. The experimental results show that Cu_3N couldn't be synthesized when other copper salts (e.g. $\text{Cu}(\text{Ac})_2$, CuCl_2 , or CuSO_4) were used as reactants. When 0.3 g of $\text{Cu}(\text{Ac})_2 \cdot \text{H}_2\text{O}$ was added into 10 ml of ODA at 240 °C, a mixture of Cu and Cu_2O was produced (Fig. S9, ESI†). When $\text{CuCl}_2 \cdot 2\text{H}_2\text{O}$ was used as the reaction precursor, we couldn't obtain any products. Because it is very difficult for Cl^- to offer electrons, ODA couldn't be compensated if it offers electrons to Cu^{2+} . Thus CuCl_2 didn't react in ODA solvent. When $\text{CuSO}_4 \cdot 5\text{H}_2\text{O}$ was used as the reactant, Cu_2S could be synthesized (eqn (6)). The formation process of Cu_2S in an ODA system is similar to that of Cu_3N . The XRD experiment (Fig. S1, ESI†) confirms the formation of Cu_2S in our synthesis. The series of Bragg reflections in XRD pattern correspond to hexagonal phase

Cu_2S (JCPDS 26-1116). Fig. 3 shows TEM, HRTEM, and SAED results of as-prepared Cu_2S . We can see from Fig. 3a that nearly monodisperse Cu_2S nanoparticles with an average diameter of 10 nm were produced. Fig. 3c reveals clear lattice fringes with an interplanar distance of about 0.34 nm which is a characteristic of the hexagonal Cu_2S crystal phase in the (002) plane. The EDS result further confirms the composition of the product (Fig. S10, ESI†). Only Cu and S peaks are observed from the EDS spectrum together with the Mo peak which was generated by the molybdenum grid.



In summary, this work presents a successful synthesis of Cu-based (Cu, Cu_3N , Cu_2O , Cu_2S) nanocrystals through direct thermal decomposition of $\text{Cu}(\text{NO}_3)_2$ and CuSO_4 in ODA solvent respectively. In this ODA synthetic system, Cu_3N and Cu_2S are the decomposed products of $\text{Cu}(\text{NO}_3)_2$ and CuSO_4 , respectively, which is very difficult to be achieved through solid state processes or other solution routes. Furthermore, the size and morphology of nanocrystals can be well controlled, which is very significant for their subsequent practical applications.

Financial support of this work by the State Key Project of Fundamental Research for Nanoscience and Nanotechnology (2011CB932401), NSFC (20921001, 21051001) and China Postdoctoral Science Foundation (20100470335) is gratefully acknowledged.

Notes and references

- 1 C. B. Murray, C. R. Kagan and M. G. Bawendi, *Annu. Rev. Mater. Sci.*, 2000, **30**, 545.
- 2 M. A. El-Sayed, *Acc. Chem. Res.*, 2004, **37**, 326.
- 3 M. B. Sigman, A. Ghezlbash, T. Hanrath, A. E. Saunders, F. Lee and B. A. Korgel, *J. Am. Chem. Soc.*, 2003, **125**, 16050.
- 4 H. Koga, T. Kitaoka and H. Wariishi, *Chem. Commun.*, 2008, 5616.
- 5 L. Guan, H. Pang, J. Wang, Q. Lu, J. Yin and F. Gao, *Chem. Commun.*, 2010, **46**, 7022.
- 6 H. Lee, S. W. Yoon, E. J. Kim and J. Park, *Nano Lett.*, 2007, **7**, 778.
- 7 M. Asano, K. Umeda and A. Tasaki, *Jpn. J. Appl. Phys.*, 1990, **29**, 1985.
- 8 Z. Q. Liu, W. J. Wang, T. M. Wang, S. Chao and S. K. Zheng, *Thin Solid Films*, 1998, **325**, 55.
- 9 K. J. Kim, J. H. Kim and J. H. Kang, *J. Cryst. Growth*, 2001, **222**, 767.
- 10 T. Nosaka, M. Yoshitake, A. Okamoto, S. Ogawa and Y. Nakayama, *Appl. Surf. Sci.*, 2001, **169**, 358.
- 11 T. Maruyama and T. Morishita, *Appl. Phys. Lett.*, 1996, **69**, 890.
- 12 F. Gulo, A. Simon, J. Kohler and R. K. Kremer, *Angew. Chem., Int. Ed.*, 2004, **43**, 2032.
- 13 J. F. Pierson, D. Wiederkehr and A. Billard, *Thin Solid Films*, 2005, **478**, 196.
- 14 J. Wang, J. T. Chen, X. M. Yuan, Z. G. Wu, B. B. Miao and P. X. Yan, *J. Cryst. Growth*, 2006, **286**, 407.
- 15 J. Choi and E. G. Gillan, *Inorg. Chem.*, 2005, **44**, 7385.
- 16 H. Zheng, R. K. Smith, Y. Jun, C. Kisielowski, U. Dahmen and A. P. Alivisatos, *Science*, 2009, **324**, 1309.
- 17 D. S. Wang, T. Xie, Q. Peng and Y. D. Li, *J. Am. Chem. Soc.*, 2008, **130**, 4016.
- 18 D. S. Wang, T. Xie, Q. Peng and Y. D. Li, *Chem.–Eur. J.*, 2008, **14**, 2507.
- 19 L. Pauling, *J. Am. Chem. Soc.*, 1932, **54**, 3570.